Analysis of the environmental conditions at Gale Crater from MSL/REMS measurements

Germán MARTÍNEZ[1], Manuel de la TORRE-JUÁREZ[2], Álvaro VICENTE-RETORTILLO[3], Osku KEMPPINEN[4], Nilton RENNO[1] and Mark LEMMON[5]

[1]Department of Climate and Space Sciences and Engineering, University of Michigan, Ann Arbor, MI, USA, gemartin@umich.edu. [2]Jet Propulsion Laboratory, California Institute of Technology, 4800 Oak Grove Drive, Pasadena, CA 91109, USA, mtj@jpl.nasa.gov. [3]Departamento de Física de la Tierra, Astronomía y Astrofísica II, Universidad Complutense de Madrid, Madrid, Spain, alvarodv@ucm.es. [4]Earth Observation, Finnish Meteorological Institute, Erik Palménin aukio 1, Helsinki, Finland, Osku.Kemppinen@fmi.fi. [5]Department of Atmospheric Sciences, Texas A&M University, College Station, TX 77843-3150, USA, lemmon@tamu.edu.

Recibido: 03/04/2016
Aceptado: 29/08/2016

Abstract
The environmental conditions at Gale Crater during the first 1160 sols of the Mars Science Laboratory (MSL) mission are assessed using measurements taken by the Rover Environmental Monitoring Station (REMS) on-board the MSL Curiosity rover. REMS is a suite of sensors developed to assess the environmental conditions along the rover traverse. In particular, REMS has been measuring atmospheric pressure, atmospheric and ground temperature, relative humidity, UV radiation flux and wind speed. Here we analyze processed data with the highest confidence possible of atmospheric pressure, atmospheric and ground temperature and relative humidity. In addition, we estimate the daily UV irradiation at the surface of Gale Crater using dust opacity values derived from the Mastcam instrument. REMS is still in operation, but it has already provided the most comprehensive coverage of surface environmental conditions recorded by a spacecraft landed on Mars.
Key words: Mars; Atmosphere; Gale Crater; Climate; MSL; REMS.

Análisis de las condiciones ambientales en el cráter Gale a partir de mediciones REMS/MSL

Resumen
En este artículo analizamos las condiciones ambientales en el cráter Gale durante los primeros 1160 soles de la misión Mars Science Laboratory (MSL). Para ello utilizamos mediciones del instrumento Rover Environmental Monitoring Station (REMS) a bordo del MSL Curiosity rover. REMS es un conjunto de sensores desarrollado para evaluar las condiciones ambientales a lo largo del trayecto del Curiosity. En particular, REMS ha estado midiendo la presión atmosférica, temperatura atmosférica y del suelo, humedad relativa, flujo de radiación UV y velocidad del viento. En este artículo analizamos datos procesados de la máxima confianza posible de presión atmosférica, temperatura del aire y del suelo y humedad relativa. Además, calculamos la irradiación UV diaria en la superficie del cráter Gale a partir de valores de opacidad del polvo obtenidos por el instrumento Mastcam. El instrumento REMS continúa activo y ya ha proporcionado el conjunto de medidas ambientales en superficie más completo registrado desde la superficie de Marte por cualquier misión espacial
Palabras clave: Marte; Atmósfera de Marte; Cráter Gale; Clima; MS; REMS.

Normalized Reference
Martínez, G., de la Torre-Juárez, M., Vicente-Retortillo, A., Kemppinen, O., Renno, N., Lemmon, M., (2016). An overview of the environmental conditions at Gale Crater from MSL/REMS measurements, *Física de la Tierra*, Vol., 28, 163-179.

Introduction

The Mars Science Laboratory (MSL) mission was launched on November 26, 2011 and landed on the floor of Gale Crater (4.6°S, 137°E) on August 5, 2012. The main objective of the MSL mission is to assess whether Mars ever had an environment capable of supporting microbial life (Grotzinger et al., 2012). MSL's Curiosity rover was sent to Gale Crater because data from the 2006 Mars Reconnaissance Orbiter indicated that it had extraordinary attributes related to the habitability of Mars (Zurek and Smrekar, 2007).

Prior to the Curiosity rover, seven spacecraft have returned data from the surface of Mars: the Viking Landers 1 and 2 in 1976, the Pathfinder in 1997, the Mars Exploration Rovers 1 and 2 in 2004 and the Phoenix lander in 2008. Many other Mars missions are expected in the next few decades, with three landers (ESA/Russia's Schiaparelli in 2016, NASA's InSight in 2018 and ESA/Russia's ExoMars in 2020), two rovers (ESA/Russia's ExoMars in 2020 and NASA's Mars2020 in 2020) and one orbiter (ESA's ExoMars in 2016) scheduled for launch in the next five years. Furthermore, human exploration is expected to occur in the next few decades.

The Curiosity rover carries the most capable suite of scientific instruments ever sent to the surface of another planet (Grotzinger et al., 2012). Curiosity is equipped with 10 science instruments, including two contact science instruments, the Alpha-Particle X-ray Spectrometer (APXS) and the Mars hand Lens Imager (MAHLI), two remote sensing instruments, the Laser-Induced Remote Sensing for Chemistry (ChemCam) and the Mars Cameras (Mastcam), two analytical laboratory instruments, the Chemistry and Mineralogy (CheMin) and the Sample Analysis at Mars (SAM) and four environmental instruments, the Dynamic Albedo of Neutrons (DAN), the Mars Descent Imager (MARDI), the Radiation Assessment Detector (RAD) and the Rover Environmental Monitoring Station (REMS).

The REMS instrument was designed to investigate the environmental conditions relevant to current habitability, such as the thermal environment, atmospheric water cycle and downward ultraviolet irradiation fluxes (Gómez-Elvira et al., 2012). To investigate such factors, REMS has been measuring atmospheric pressure, atmospheric relative humidity, ground and atmospheric temperatures, UV radiation fluxes and horizontal wind speeds. In this article, we analyze the environmental conditions at

Gale Crater based on REMS measurements during the first 1160 sols of the MSL mission.

Section 2 of this article provides a comprehensive overview of the REMS instrument, with detailed information about the different sensors comprising REMS. Section 3 discusses processed data with the highest quality of atmospheric pressure, ground and air temperature and relative humidity. It also discusses numerically-calculated values of the daily UV irradiation at the MSL landing site using dust opacity values measured by Mastcam. Finally, section 4 provides a summary of this article.

1. The Rover Environmental Monitoring Station

The REMS instrument includes 6 different sensors that measure atmospheric pressure (P), atmospheric relative humidity (RH), ground temperature (T_g), atmospheric temperature (T_a), UV radiation fluxes and horizontal wind speed (Gómez-Elvira et al., 2012, 2014). These sensors are located on two booms on the MSL Remote Sensing Mast, on the rover deck and inside the rover body, as shown in Fig. 1.

The pressure sensor (PS) is located in the rover body inside the Instrument Control Unit (ICU) that provides the interface with the rover. The pressure sensor is based on piezoelectric capacitor plates with extensive flight heritage (Mars 96, Mars Polar Lander, Beagle 2 and Phoenix) (Harri et al., 2014a). The ground temperature sensor (GTS) is mounted on boom 1 and measures the intensity of infrared radiation emitted by the ground in the bandwidths 8-14, 15.5-19 and 14.5-15.5 μm. The GTS uses three thermopiles pointed 26° downward from the plane of the rover deck with a field of view (FOV) of 60° horizontally and 40° vertically, covering a ground area of about 100 m^2 depending on the angle between the surface and sensor (Sebastián et al., 2010). Air temperature sensors (ATS) are located on the two booms, at approximately 1.6 m height. They are based on thermistors because of their robustness, with a typical response time less than 1 s. The relative humidity sensor (RHS) is located on boom 2 at about 1.6 m height. It is based on an active polymer film that changes its capacitance a function of the relative humidity (Harri et al., 2014b). The ultraviolet sensor (UVS) is located on the rover deck and is comprised of six photodiodes to measure the UV flux in different bands, one global in the range 200-380 nm named ABC and 5 filtered photodiodes in the range 320-380, 280-320, 200-280, 230-290 and 350 nm named A, B, C, D and E, respectively.

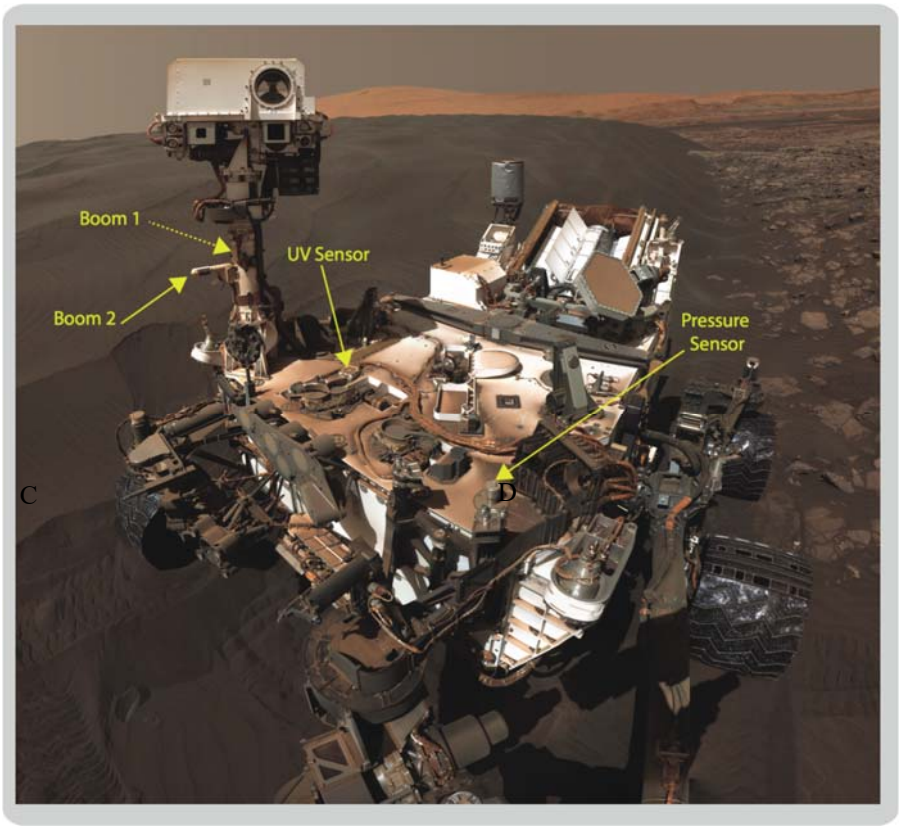

Figure 1. Location of REMS sensors on the Curiosity Rover. The RHS is located on boom 1, the GTS is located on boom 2 and the ATS and WS are located on both booms. Note that boom 1 is hidden behind the mast. The UVS and PS are located on the rover deck.

The REMS-UV sensor is placed on the rover deck, facing the sky with a nominal field of view of 30°. The FOV is geometrically limited by the photodiode caging. Due to its location, the sensor is exposed to dust deposition and design constraints ruled out any active protection system. In order to mitigate the dust degradation effect, a magnet was placed around each photodiode to create a magnetic field to deflect dust. Finally, the wind sensor (WS) uses hot wire anemometry to record the wind speed, following the Viking design. The range, resolution and accuracy of REMS sensors are shown in Table 1.

Table 1. Calibration range, accuracy and resolution of REMS sensors (Gómez-Elvira et al., 2012).

	Range	Accuracy	Resolution
P (Pa)	0-1400	< 2 .7	0.2
T_g (K)	150-300	< 10	2
T_a (K)	150-300	< 5	< 0.1
RH (%)	0-100	2, T > 243 K 10, 203 < T < 243 K 20, T < 203 K	< 0.1
UV_{ABC}; UV_A; UV_B; UV_D; UV_E (W/m^2)	56.9; 25; 9.5; 1.57; 5; 10.6	< 5%	< 0.5%

REMS has been complementing and extending the scientific return of previous meteorological stations sent to Mars. In particular, REMS is measuring UV radiation flux at the Martian surface for the first time, while it is significantly improving our knowledge of ground temperature variations. This type of measurement was pioneered by the Mini-TES aboard the MERs (Spanovich et al., 2006) and is being extended by the REMS GTS, which is providing more continuous and systematic measurements than ever before. In addition, REMS is expanding the spatial and temporal coverage of environmental quantities previously measured at the surface of Mars by recording the atmospheric pressure, relative humidity, atmospheric temperature and wind speed at equatorial latitudes. Table 2 shows a summary of the different environmental quantities measured by the different instrument sent to Mars, along with their temporal coverage.

2. Environmental conditions at Gale Crater

In this section we analyze the environmental conditions at Gale Crater during the first 1160 sols of the MSL mission. We show REMS data processed with the highest confidence. In addition, we estimate the daily UV irradiation using dust opacity values derived from the Mastcam instrument.

Table 2. Environmental quantities measured by the different environmental instrument sent to Mars, along with their time coverage. The Sols column shows the number of Sols for which data are available in the NASA Planetary Data System, while MY stands for Martian year. 'Pulled' means that the data were removed from the NASA PDS due to calibration issues.

Mission	Lat (°)	Instrument	Quantities	Height (m)	Sols	MY
VL1	22.5N	VMIS	P,T_a,u,v	1.6	2245	12-15
VL2	48.5N	VMIS	P,T_a,u,v	1.6	1050	12-13
PF	19.7N	ASI/MET	P T_a u,v	0.3 0.52,0.77,1.27 1.31	83 83 Pulled	23
MER-1	1.9S	MiniTES	T Profile	20-2000	2243	26-29
MER-2	14.6S	MiniTES	T Profile	20-2000	2174	26-29
PHO	68.2N	MET TECP	T_a P u,v Dust&Ice RH T_g	1.25, 15,2 1 2 250-20000 0.03-2.27 --	150 Pulled	29
MSL	4.5S	REMS	T_a,u,v,RH P, UV T_g	1.5 Deck --	In Progress	31-32

.

The nominal strategy for REMS data acquisition consists of 5 minutes of measurements at 1 Hz every Mars hour, with at least an additional hour of 1 Hz measurement during every sol. Given additional available payload energy, the team decided to extend REMS measurements coverage by using the so-called extended blocks, which replace the nominal 5-minute blocks by blocks lasting one or more hours. The extended blocks allow for a much better data coverage of events of the time scale of minutes to hours, improving the probability of capturing transient phenomena such as dust devils and evening boundary layer oscillations.

2.1. Atmospheric Pressure

We calculate high-quality hourly values of atmospheric pressure by averaging REMS/PS measurements with the highest confidence taken nominally during the first five minutes of each hour. We show in Fig. 2 daily maximum and minimum pressure values during the first 1160 sols of the MSL mission. The main contribution to the large annual variability in surface pressure shown in Fig. 2 is caused by the release and capture of CO_2 by the polar caps. During the spring season in the southern hemisphere, parts of the southern polar cap sublimate and the released CO_2 gas increases the atmospheric pressure with an annual maximum occurring in late spring at a solar longitude $L_s \sim 250°$. Then, during the cold season in the southern hemisphere, the released CO_2 gas is deposited back in southern polar cap with an annual minimum occurring in late winter at $L_s \sim 157°$. The relative minimum in late summer ($L_s \sim 344°$) and relative maximum in late fall ($L_s \sim 57°$) are caused by the deposition and sublimation of CO_2 onto and from the northern polar cap, respectively.

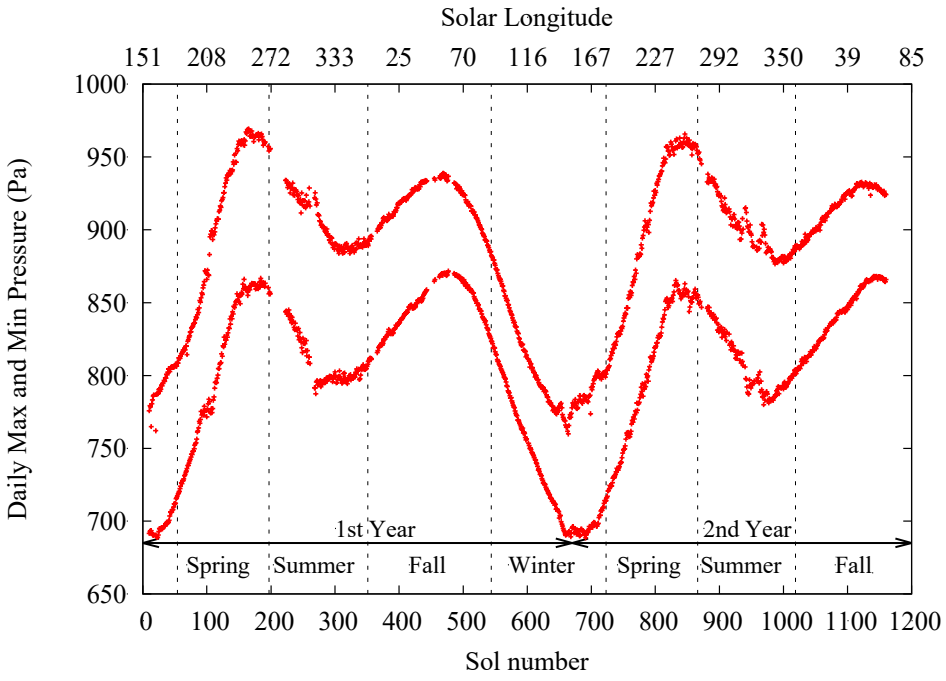

Figure 2. Inter-annual evolution of the surface pressure at the MSL landing site during the first 1160 sols of the mission measured by the REMS/PS.

The diurnal amplitude in pressure is stronger than measured during past missions. This is explained by the fact that MSL is at a lower elevation than earlier missions, such as the Viking Landers. The lower elevation causes a larger amount of atmos-

pheric mass to be on top of the instrument, causing larger surface pressure. As the diurnal variation due to changes in the temperature of the atmospheric gas is proportional to the total pressure, the diurnal variation measured by REMS is larger than those measured by previous missions.

2.2. Surface Irradiance

We use a comprehensive spectral radiative transfer model along with aerosol optical depth (τ) values derived from the Mastcam instrument to calculate the daily UV irradiation at the surface of Gale Crater during the first 1160 sols of the MSL mission. The daily UV irradiation represents the total amount of UV energy received during one sol and is an important quantity because it might constrain the existence of microbial habitats on the surface and shallow subsurface of Mars (Cockell and Raven, 2004). We have not used measurements by REMS to calculate the daily UV irradiation because the limited FOV of the UVS does not allow capturing all incoming solar radiation.

Our radiative transfer model includes up-to-date wavelength-dependent radiative properties of dust, water ice clouds and gas molecules (Vicente-Retortillo et al., 2015). It enables the characterization of the radiative environment under different environmental scenarios and locations by modifying a number of input parameters such as dust optical depth at 880 nm, solar longitude, latitude, spectral band and the wavelength-dependent values of extinction efficiency, single scattering albedo and asymmetry factor. Among these parameters, the dust optical depth at 880 nm has the strongest impact on calculated surface irradiances. We use optical depth values referenced to the 880 nm value derived from direct imaging of the Sun by Mastcam (e.g., Lemmon et al., 2015). Mastcam images of the Sun are nominally taken every three to seven sols.

We show in Fig. 3 values of the daily UV irradiation at the top of the atmosphere (TOA) and at the surface of Gale Crater, along with Mastcam τ values. The seasonal evolution of the daily irradiation at the surface departs from that at the TOA because the solar radiation interacts with atmospheric aerosols by means of absorption and scattering processes. When the irradiation at the TOA shows the annual minimum value (late fall, $L_s \sim 80°$), the aerosol optical depth is low (~0.4) and the irradiation at the surface follows that at the TOA, showing an annual minimum as well. However,

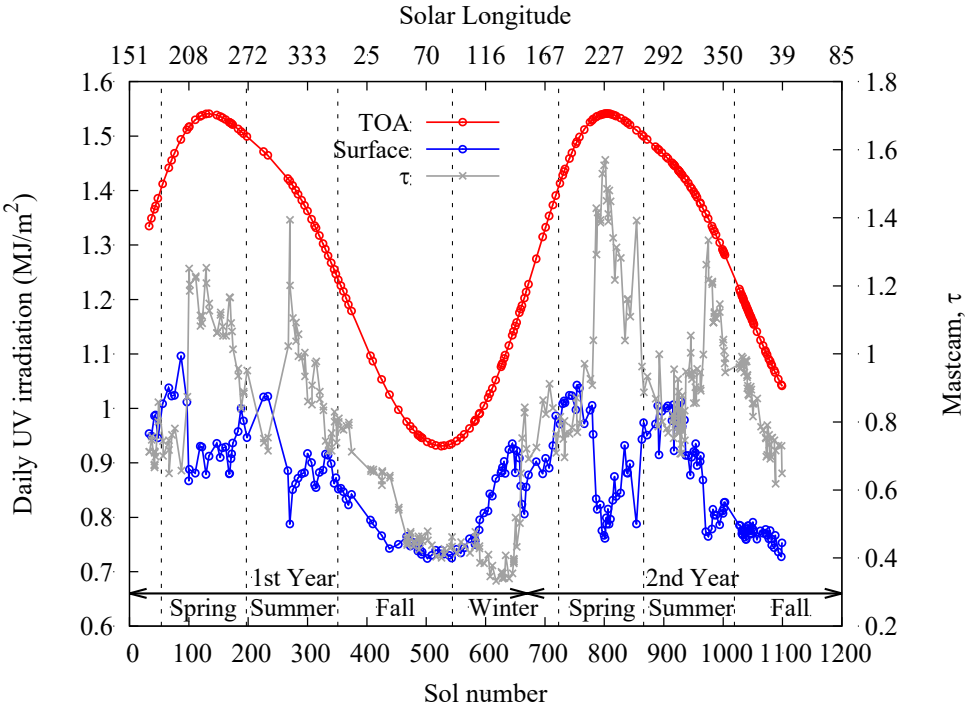

Figure 3. Inter-annual evolution of the daily UV irradiation at the TOA (black solid circles) and at the surface of Gale Crater (black empty circles), along with aerosol optical depth values (grey crosses) derived from Mastcam images of the Sun. Values of the daily UV irradiation at the surface have been calculated using a comprehensive radiative transfer model presented in Vicente-Retortillo et al. (2015).

when the irradiation at the TOA shows the annual maximum value (middle spring, L_s ~ 230°), the irradiation at the surface does not show a corresponding annual maximum. This is because at this time the aerosol optical depth shows a relative maximum (τ ~1.25 during the first year, and τ ~1.6 during the second), with about 50% of the irradiation at the TOA being absorbed and scattered before reaching the surface.

During the first and second year, the irradiation at the surface shows two relative maxima in early spring and summer (L_s ~ 208° and 292°; Fig. 3). This is because the aerosol optical depth presents two relative minima at these times, with the irradiation at the TOA showing values close to the annual maximum (L_s ~ 230°). A companion paper in this issue (Vicente-Retortillo, 2016) provides more detailed characterization of the radiative environment at Gale Crater.

2.3. Near-surface air and ground temperature

We calculate high-quality hourly values of ground temperature by averaging REMS/GTS measurements with the highest confidence nominally taken during the first five minutes of each hour. That is, we only use GTS measurements with the ASIC power supply in range, the highest recalibration quality and with no shadows in the GTS FOV to maximize the sensor performance. Similarly, we calculate hourly values of air temperature at 1.6 m by averaging reliable ATS measurements taken nominally during the first five minutes of each hour. Since the ATS is subject to thermal contamination from the radioactive thermal generator and waste heat from the rover, the interpretation of ATS measurements as an environmental temperature must be carefully taken.

We show in Fig. 4 daily maximum and minimum values of air and ground temperature during the first 1160 sols of the MSL mission. To a first approximation, the ground temperature follows the seasonal evolution of the irradiation at the surface (Fig. 3), with the lowest annual T_g values occurring in late fall and early winter and the highest T_g values occurring in spring and summer. The annual minimum ground temperature (~173 K) occurred at Dingo Gap during late fall on sol 534 (L_s = 85°), while on the other extreme the annual maximum ground temperature (~289 K) occurred during late southern hemisphere winter and early spring on sols 103 and 711 (L_s = 210° and 174°).

The diurnal amplitude in ground temperature (difference between the maximum and minimum value of T_g on a certain sol) varies with the time of the year (Fig. 4), with values ranging from about 55 K around sol 1120 (L_s ~ 48°) to 100 K around sol 710 (L_s ~ 173°). This quantity is mostly affected by the type of terrain and in particular by its thermal inertia (I), which regulates thermal excursions of ground temperatures at diurnal and seasonal timescales. For a given irradiation, terrains with low values of thermal inertia feature warmer daytime maximum temperatures and colder nighttime minimum temperatures than terrains with higher I values. As an example, the sudden decrease in the diurnal maximum ground temperature occurred on sol 120 (Fig. 4; L_s ~220°) coincided with the rover's traverse from a terrain with I ~300 S.I. to another terrain (Yellowknife Bay) with I ~ 420 S.I. (Martinez et al., 2014).

Changes in dust opacity also regulate thermal excursions of ground temperature (e.g. Määttänen and Savijärvi, 2004). For a given type of terrain, low τ values cause warmer daytime maximum temperatures and colder nighttime minimum temperatures than higher τ values do (as thermal inertia). This is because dust readily absorbs solar

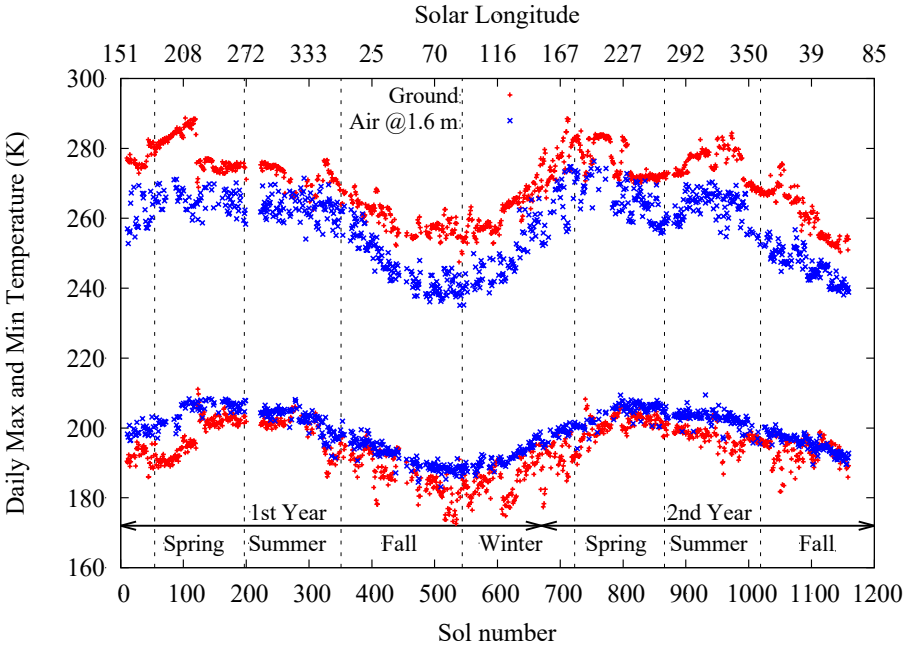

Figure 4. Inter-annual evolution of the ground (black solid circles) and air temperature (grey crosses) at the MSL landing site during the first 1160 sols of the mission measured by the REMS GTS and ATS.

radiation during the daytime, reducing the insolation at the surface. At night, though, downward infrared emission from aerosols warms the ground. However, the effect of dust opacity on changes in the diurnal amplitude of ground temperature is not apparent at Gale Crater, where sudden increases in dust opacity are not necessarily followed by a reduction in the diurnal amplitude in ground temperature. For instance, the sudden increase in aerosol optical depth at $L_s \sim 208°$ during the first year (Fig. 3) was not followed by a decrease in the daily maximum ground temperature (Fig. 4). A more detailed quantification of the impact of I and τ on changes in ground temperature is left as future work.

The seasonal evolution of the near-surface air temperature is also shown in Fig. 4. It follows the seasonal evolution of the ground temperature, although with lower diurnal amplitudes ranging from ~45 K around sol 550 ($L_s \sim 93°$) to ~75 K around sol 710 ($L_s \sim 173°$). Maximum daily values of T_a are usually achieved between 14:00 and 16:00 LTST, approximately about two hours after the peak in T_g. At night, minimum daily T_a values are generally achieved between 05:00 and 07:00 LTST, one to two hours after the minimum in T_g depending on the time of the season. Further details on

the diurnal evolution of the near-surface air and ground temperatures are given in a companion paper in this issue (Pla-García and Rafkin, 2016).

2.4. Near-surface humidity

We calculate high-quality hourly values of *RH* by selecting RHS measurements obtained with the latest recalibration parameters and taken only during the first four seconds of measurements after the RHS has been turned on after ~5 min of inactivity to avoid heating on the sensor. These values include *RH* measurements taken during the nominal and the so-called high-resolution interval mode (HRIM). The HRIM measurement strategy consists of alternately switching on and off the sensor at periodic intervals to minimize heating and is only used on selected ~one-two-hour long observations. Fig. 5 shows an example of the RHS measuring strategy on sol 1137, with *RH* values with the highest confidence highlighted in black.

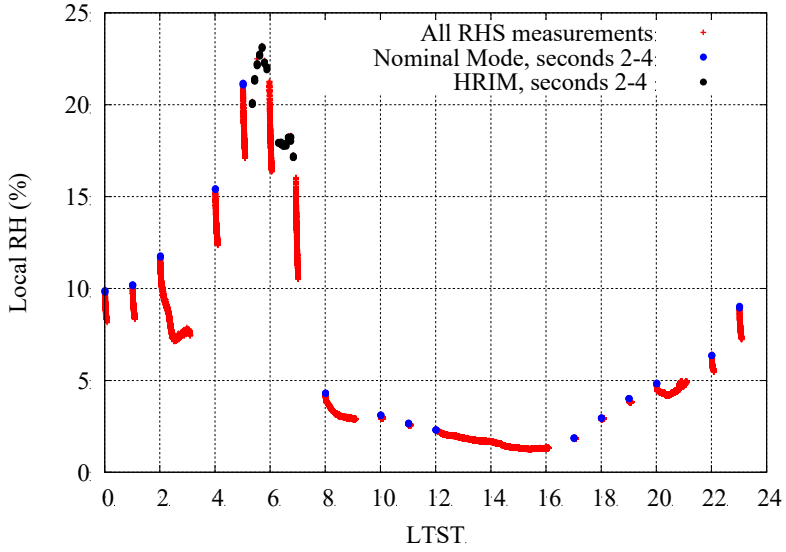

Figure 5. Example of RHS measurement strategy on sol 1137. Grey crosses represent the complete set of RHS measurements. Black solid circles represent RHS measurements obtained in the nominal mode but only during seconds 2, 3 and 4 after the RHS has been turned on after ~5 min of inactivity. Black triangles represent *RH* measurements obtained during seconds 2, 3 and 4 in the HRIM mode. Note that *RH* values rapidly decrease due to spurious effects of heating, as clearly indicated by the sudden drops in *RH* values (grey crosses). In this study, we only use RHS measurement with the highest confidence (black solid circles and triangles).

Using *RH* measurements selected as described above, we show the daily maximum *RH* value during the first 1160 sols of the MSL mission in Fig. 6. We also show corresponding values of the volume mixing ratio (*VMR*) derived from simultaneous

REMS measurements of *RH*, *T* and *P* as $VMR = RH \times e_s(T)/P$, where e_s is the saturation vapor pressure over ice. The *RH* showed the highest annual values around early winter, with values ~70% on sol 551 (L_s ~ 93°), and the lowest annual values around late spring and early summer, with values below 10%. Unlike at the Phoenix landing site (Whiteway et al., 2009), near-surface fog did not form at Gale Crater because *RH* values stay well below saturation levels. However, the nighttime and early morning ground temperature can be as much as ~15 K colder than that at 1.6 m above the surface (Fig. 4), allowing the ground to reach the frost point temperature on a few sols (Martínez et al., 2015; Savijärvi et al., 2015a).

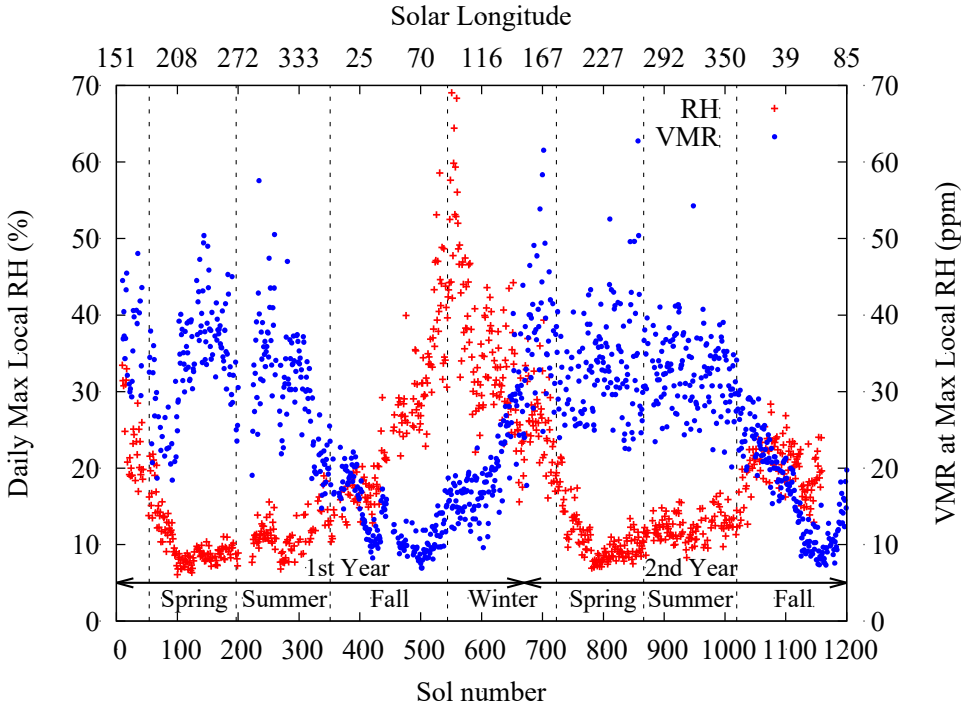

Figure 6. Inter-annual evolution of the maximum relative humidity per sol (black pluses), generally achieved between 04:00 and 06:00 LTST, and corresponding value of volume mixing ratio (grey crosses) derived from simultaneous measurements by the PS and RHS.

The seasonal evolution of relative humidity is mainly controlled by temperature (not by atmospheric water content) at the Curiosity's landing site. The diurnal maximum value of *RH* usually occurs at the same time as the minimum diurnal value of T_g (between 04:00 and 06:00 LTST). Therefore, the maximum diurnal value of *RH* shown in Fig. 6 follows the minimum diurnal value of T_g shown Fig. 4. Interestingly, the seasonal evolution of the daily maximum *RH* appears to be anti-correlated with

that of the near-surface *VMR* (Fig. 6). The lowest annual values of *VMR* occur in late fall and winter, when the daily maximum *RH* is the highest. Similarly, the highest annual values of *VMR* occur in late winter, spring and early summer, when the daily maximum *RH* is the lowest.

The sol-to-sol variability in *VMR* seems to be larger in spring and summer than in late fall and winter (Fig. 6). There is a chance that this variability may be related to the uncertainty in *VMR* values rather than to actual variations in *VMR*. This is because the most accurate daily *VMR* value is derived when the relative humidity is the highest. Therefore, *VMR* values derived in spring and summer, when the diurnal maximum *RH* is low, present higher uncertainties that *VMR* values derived in late fall and winter, when the diurnal maximum *RH* is the highest. Independent estimations of near-surface *VMR* values from daytime ChemCam passive sky measurements can further constrain the sol-to-sol variability in *VMR* at Gale Crater.

3. Summary

We have presented a brief summary of processed REMS measurements of atmospheric pressure, atmospheric and ground temperature and relative humidity to give an overview of the environmental conditions at Gale Crater. We have also estimated the daily UV irradiation using dust opacity values derived from the Mastcam instrument. For more specific information on scientific results obtained from the different REMS sensors, the reader is referred to Harri et al. (2014a), Haberle et al. (2014), Kahanpää et al. (2016) and Guzewich et al. (2016) for the PS; Hamilton et al. (2014), Martínez et al. (2014) and Martínez et al. (2015) for the GTS; Harri et al. (2014b), Martín-Torres et al. (2015), Savijärvi et al. (2015a), Martínez et al. (2015) and Savijärvi et al. (2015b) for the RHS and Smith et al. (2016) for the UVS. REMS has already provided the most comprehensive coverage of near-surface environmental conditions recorded by a spacecraft landed on Mars.

Acknowledgments

This research is supported by JPL grant number 1449038. We would like to thank Erik Fischer for his contribution to improve this article. We also thank the REMS Team for their support of this investigation.

References

COCKELL, C.S., RAVEN, J.A. (2004). Zones of photosynthetic potential on Mars and the early Earth. *Icarus*, 169(2), 300-310. doi:10.1016/j.icarus.2003.12.024.

GROTZINGER, J.P., CRISP, J., VASAVADA, A.R., ANDERSON, R.C., BAKER, C.J., BARRY, R., BLAKE, D.F., CONRAD, P., EDGETT, K.S., FERDOWSKI,

B., GELLERT, R. (2012). Mars Science Laboratory mission and science investigation. *Space. Sci. Rev.*, 170(1-4), pp.5-56. doi: 10.1007/s11214-012-9892-2.

HABERLE, R.M., GÓMEZ-ELVIRA, J., TORRE-JUÁREZ, M.D.L., HARRI, A.M., HOLLONGSWORTH, J.L., KAHANPÄÄ, H., KAHRE, M.A., LEMMON, M., MARTÍN-TORRES, F.J., MISCHNA, M., MOORES, J.E. (2014). Preliminary interpretation of the REMS pressure data from the first 100 sols of the MSL mission. *J. Geophys. Res. Planets*, 119(3), 440-453. doi: 10.1002/2013JE004488.

HAMILTON, V.E., VASAVADA, A.R., SEBASTIÁN, E., TORRE-JUÁREZ, M., RAMOS, M., ARMIENS, C., ARVIDSON, R.E., CARRASCO, I., CHRISTENSEN, P.R., DE PABLO, M.A., GOETZ, W. (2014). Observations and preliminary science results from the first 100 sols of MSL Rover Environmental Monitoring Station ground temperature sensor measurements at Gale Crater. *J. Geophys. Res. Planets*, 119, 745–770, doi: 10.1002/2013JE004520.

HARRI, A.M., GENZER, M., KEMPPINEN, O., KAHANPÄÄ, H., GÓMEZ-ELVIRA, J., RODRÍGUEZ-MANFREDI, J.A., HABERLE, R., POLKKO, J., SCHMIDT, W., SAVIJÄRVI, H., KAUHANEN, J. (2014a). Pressure observations by the Curiosity rover: Initial results. *J. Geophys. Res. Planets*, 119(1), 82-92. doi: 10.1002/2013JE004423.

HARRI, A.M., GENZER, M., KEMPPINEN, O., GÓMEZ-ELVIRA, J., HABERLE, R., POLKKO, J., SAVIJÄRVI, H., RENNO, N., RODRÍGUEZ-MANFREDI, J.A., SCHMIDT, W., RICHARDSON, M. (2014b). Mars Science Laboratory relative humidity observations: Initial results. *J. Geophys. Res. Planets*, 119, 2132–2147, doi: 10.1002/2013JE004514.

GUZEWICH, S.D., NEWMAN, C.E., TORRE-JUÁREZ, M., WILSON, R.J., LEMMON, M., SMITH, M.D., KAHANPÄÄ, H. and HARRI, A.M. (2016). Atmospheric tides in Gale Crater, Mars. *Icarus* 268, 37-49. doi:10.1016/j.icarus.2015.12.028.

GÓMEZ-ELVIRA, J., ARMIENS, C., CARRASCO, I., GENZER, M., GÓMEZ, F., HABERLE, R., HAMILTON, V.E., HARRI, A.M., KAHANPÄÄ, H., KEMPPINEN, O., LEPINETTE, A. (2014). Curiosity's rover environmental monitoring station: Overview of the first 100 sols. *J. Geophys. Res. Planets*, 119 (7), 1680–1688. doi: 10.1002/2013JE004576.

GÓMEZ-ELVIRA, J., ARMIENS, C., CASTAÑER, L., DOMÍNGUEZ, M., GENZER, M., GÓMEZ, F., HABERLE, R., HARRI, A.M., JIMÉNEZ, V., KAHANPÄÄ, H. KOWALSKI, L. (2012). REMS: The environmental sensor suite for the Mars Science Laboratory rover. *Space Sci. Rev*. 170 (1-4), 583-640. doi: 10.1007/s11214-012-9921-1.

KAHANPÄÄ, H., NEWMAN, C., MOORES, J., ZORZANO, M.P., MARTÍN-TORRES, J., NAVARRO, S., LEPINETTE, A., CANTOR, B., LEMMON, M.T., VALENTÍN-SERRANO, P. and ULLÁN, A. (2016). Convective vortices and dust

devils at the MSL landing site: Annual variability. *J. Geophys. Res.: Planets*, 21(8), 1514-1549. doi: 10.1002/2016JE005027.

LEMMON, M.T., WOLFF, M.J., BELL, J.F., SMITH, M.D., CANTOR, B.A. and SMITH, P.H. (2015). Dust aerosol, clouds, and the atmospheric optical depth record over 5 Mars years of the Mars Exploration Rover mission. *Icarus*, 251, 96-111. doi:10.1016/j.icarus.2014.03.029.

MÄÄTTÄNEN, A., SAVIJÄRVI, H. (2004). Sensitivity tests with a one-dimensional boundary-layer Mars model. *Bound. Lay. Meteorol*., 113(3), 305–320. doi: 10.1007/s10546-004-5274-y.

MARTÍN-TORRES et al. (2015). Transient liquid water and water activity at Gale crater on Mars. *Nat. Geosci.*, 8, 357-361. doi: 10.1038/ngeo2412.

MARTÍNEZ, G.M., RENNO, N., FISCHER, E., BORLINA, C.S., HALLET, B., TORRE-JUÁREZ, M., VASAVADA, A.R., RAMOS, M., HAMILTON, V., GÓMEZ-ELVIRA, J. and HABERLE, R.M. (2014). Surface energy budget and thermal inertia at Gale Crater: Calculations from ground-based measurements. *J. Geophys. Res. Planets* 119 (8), 1822-1838. doi: 10.1002/2014JE004618.

MARTÍNEZ, G.M., FISCHER, E., RENNO, N.O., SEBASTIÁN, E., KEMPPINEN, O., BRIDGES, N., BORLINA, C.S., MESLIN, P.Y., GENZER, M., HARRI, A.H. and VICENTE-RETORTILLO, A. (2016). Likely frost events at Gale crater: Analysis from MSL/REMS measurements. *Icarus* 280, 93-102, doi:10.1016/j.icarus.2015.12.004.

PLA-GARCÍA, J., RAFKIN, S. (2016). *Física de la Tierra* (this issue).

SAVIJÄRVI, H.I., HARRI, A.M. and KEMPPINEN, O. (2015a). Mars Science Laboratory diurnal moisture observations and column simulations. *J. Geophys. Res*. Planets 120, 1011–1021. doi: 10.1002/2014JE004732.

SAVIJÄRVI, H., HARRI, A.M. and KEMPPINEN, O. (2016). The diurnal water cycle at Curiosity: Role of exchange with the regolith. *Icarus*, 265, 63-69. doi:10.1016/j.icarus.2015.10.008.

SEBASTIÁN, E., ARMIENS, C., GÓMEZ-ELVIRA, J., ZORZANO, M.P., MARTÍNEZ-FRÍAS, J., ESTEBAN, B. and RAMOS, M. (2010). The rover environmental monitoring station ground temperature sensor: A pyrometer for measuring ground temperature on Mars. *Sensors*, 10(10), 9211-9231. doi: 10.3390/s101009211.

SMITH, M.D., ZORZANO, M.P., LEMMON, M., MARTÍN-TORRES, J. and de CAL, T.M. (2016). Aerosol optical depth as observed by the Mars Science Laboratory REMS UV photodiodes. *Icarus*, 280, 234-248. doi:10.1016/j.icarus.2016.07.012.

SPANOVICH, N., SMITH, M.D., SMITH, P.H., WOLFF, M.J., CHRISTENSEN, P.R. and SQUYRES, S.W. (2006). Surface and near-surface atmospheric temperatures from the Mars Exploration Rover landing sites. *Icarus*, 180, 314-320. doi:10.1016/j.icarus.2005.09.014.

VICENTE-RETORTILLO, A., VALERO, F., VÁZQUEZ, L. and MARTÍNEZ, G.M. (2015). A model to calculate solar radiation fluxes on the Martian surface. *J. Space Weather Space Clim*., 5, A33. doi:10.1051/swsc/2015035.

VICENTE-RETORTILLO, A., LEMMON, M., MARTÍNEZ, G.M., VALERO, F., VÁZQUEZ, MARTÍN, M.L. (2016). Seasonal and Interannual variability of solar radiation at Spirit, Opportunity and Curiosity landing sites. *Física de la Tierra* (this issue).

WHITEWAY, J.A., KOMGUEM, L., DICKINSON, C., COOK, C., ILLNICKI, M., SEABROOK, J., POPOVICI, V., DUCK, T.J., DAVY, R., TAYLOR, P.A. and PATHAK, J. (2009). Mars water-ice clouds and precipitation. *Science*, 325(5936), 68-70. doi:10.1126/science.1172344.

ZUREK, R.W., SMREKAR, S.E. (2007). An overview of the Mars Reconnaissance Orbiter (MRO) science mission. *J. Geophys. Res*. 112. E05S01. doi: 10.1029/2006JE002701